Characterisation of Self-locking High-contraction Electro-ribbon Actuators*

Majid Taghavi, Tim Helps, Jonathan Rossiter

***Abstract*— Actuators are essential devices that exert force and do work. The contraction of an actuator (how much it can shorten) is an important property that strongly influences its applications, especially in engineering and robotics. While high contractions have been achieved by thermally- or fluidically-driven technologies, electrically-driven actuators typically cannot contract by more than 50%. Recently developed electro-ribbon actuators are simple, low cost, scalable electroactive devices powered by dielectrophoretic liquid zipping (DLZ) that exhibit high efficiency (~70%), high power equivalent to mammalian muscle (~100 W/kg), contractions exceeding 99%. We characterise the electro-ribbon actuator and explore contraction variation with voltage and load. We describe the unique self-locking behaviour of the electro-ribbon actuator which could allow for low-power-consumption solenoids and valves. Finally, we show the interdependence of constituent material properties and the important role that material choice plays in maximising performance.**

I. Introduction

Actuators (such as motors and muscles) are essential devices that exert force and do work, allowing man-made and natural systems to perform useful tasks. Many actuators are tensile, exerting a tensile force when active, and shortening when doing work. Contraction (reduction in length divided by initial length) describes how much an actuator may shorten. Most actuators exhibit contractions less than 50% (Table 1, appendix), which restricts their usefulness.

Higher contractions may be achieved with thermally driven actuation technologies, such as shape-memory polymers [1], shape-memory alloy coils [2] and coiled polymers [3]; however, because of their thermal nature they are energetically inefficient (less than 10% of input thermal energy is converted to mechanical energy [4], [5]). Achieving high bandwidths in thermally driven actuators is also challenging due to thermal inertia [6], [7].

Some pneumatic actuators have been specifically designed for high contraction and can reach 65% contraction when positive pressure is applied [8], while vacuum-driven origami artificial muscles (origami structures which fold inwards while contracting) have demonstrated extremely high contractions up to 99.7% [9], [10]. While they exhibit high contractions, pneumatic actuators require large, heavy pumps or pressure vessels, and vacuum-driven fluidic actuators are fundamentally limited in actuation stress because applied pressure cannot exceed 100 kPa, atmospheric pressure (assuming a perfect vacuum within the actuator).

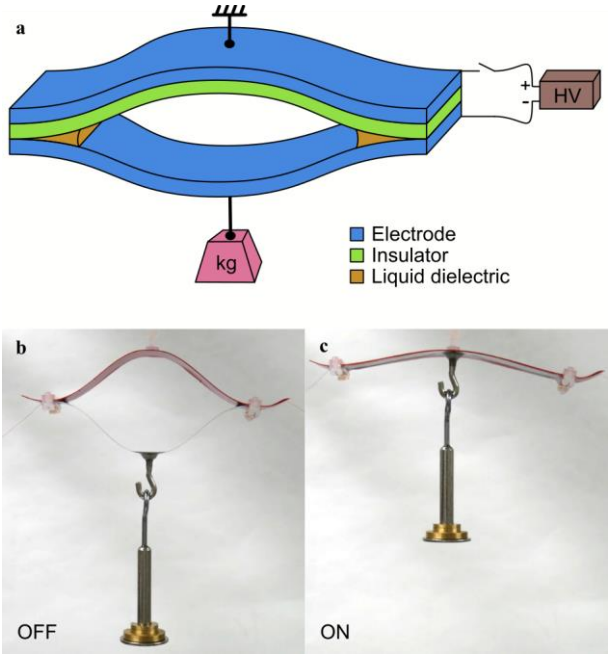

Fig. 1 Bow-shaped electro-ribbon actuators. **a**) Bow-shaped electro-ribbon actuator design. **b**) Typical bow-shaped electro-ribbon actuator, which is made from thin steel electrodes and PVC tape. **c**) Lifting an 18 g mass when 8 kV is applied.

Electrically driven actuators are often desirable because their energy source is well matched to the world's infrastructure; electrical power is readily available, while pneumatic or hydraulic devices typically use a compressor or pump to convert electrical energy to fluid pressure. The highest strains for electroactive actuators are those of single layers of dielectric elastomer actuators, which can achieve thickness strains of 79% [11], but when stacked in useful, multilayer structures, have only reached 46% [12].

Electro-ribbon actuators are a recently developed electrostatic actuator technology, which can be made from almost any combination of insulating and conductive materials and exhibit contractions up to 99.8% [13]. In addition to being electrically driven, they are simple, low cost, high efficiency,

* Majid Taghavi is supported by EPSRC grant EP/R02961X/1. T. Helps is supported by the Royal Academy of Engineering and the Office of the Chief Science Adviser for National Security under the UK Intelligence Community Postdoctoral Fellowship Programme. Jonathan Rossiter is supported by the Royal Academy of Engineering through the Chair in Emerging Technologies scheme and EPSRC grant EP/M020460/1.

M. Taghavi, T. Helps, and J. Rossiter are with the Department of Engineering Maths, University of Bristol, 75 Woodland Rd, Bristol, BS8 1UB and Bristol Robotics Laboratory, Stoke Gifford, Bristol, BS16 1QY, UK (email majid.taghavi@bristol.ac.uk tim.helps@bristol.ac.uk,, jonathan.rossiter@bristol.ac.uk).

high power, scalable actuators, making them well suited for a wide range of robotics and engineering applications.

Electro-ribbon actuators are driven by dielectrophoretic liquid zipping (DLZ). In DLZ devices, a pair of electrodes are separated by an insulator and mechanically connected at one or both ends (Fig. 1a). Mechanical connection can be achieved using a range of connection methods including adhesives, magnets, or mechanical clamping.

The electrodes are oppositely charged, causing an electric field to be developed between them, which is especially strong near the point of mechanical connection, where the electrodes are closest to one another. This point is referred to as the zipping locus. A sufficiently strong electric field will induce a strong electrostatic attractive force that causes the electrodes to progressively zip together, starting at the zipping locus. This behaviour has been captured in previous zipping devices to do useful work [14]–[16].

In DLZ devices, a small droplet of high-permittivity, high-breakdown-strength liquid dielectric is added at the zipping locus, considerably amplifying the electrostatic force developed. The overall closing force is coupled to Maxwell pressure, $P = \varepsilon E^2$, where ε is the permittivity of the liquid dielectric and E is the electric field [17]. The droplet of liquid dielectric increases electrostatic force as a result of its higher permittivity compared with air. Additionally its higher breakdown strength compared with air allows for much stronger fields to be sustained, further increasing maximum closing force by a factor of up to $\left(\frac{E_{breakdown,liquid}}{E_{breakdown,air}}\right)^2$.

Dielectrophoretic forces, which have the effect of drawing high-permittivity materials into regions of high electric field density [18], attract the liquid dielectric into the zipping locus, where it is then driven along the actuator as it progressively zips closed, continually amplifying electrostatic force as the device contracts (Fig. 1b–c).

The attractive force for an analogous system, two parallel charged plates separated by an insulator and a medium, is described by

$$F = \frac{\frac{1}{2}\varepsilon_{medium}\varepsilon_0 A V^2}{\left(\frac{\varepsilon_{medium}}{\varepsilon_{insulator}} t_{insulator} + t_{medium}\right)^2} \qquad (1)$$

where F is the attractive force; ε_{medium}, $\varepsilon_{insulator}$ and ε_0 are the permittivity of the medium, insulator and free space, respectively; A is the plate area; V is the applied voltage; and $t_{insulator}$ and t_{medium} are the insulator and medium thickness, respectively [13]. In the case of electro-ribbon actuators, the liquid dielectric is the medium.

In this article, we present further characterisation and analysis of electro-ribbon actuators. We examine their contraction as a function of applied voltage and load, explore the self-locking capabilities of electro-ribbon actuators, and investigate how the insulator and liquid dielectric materials affect performance.

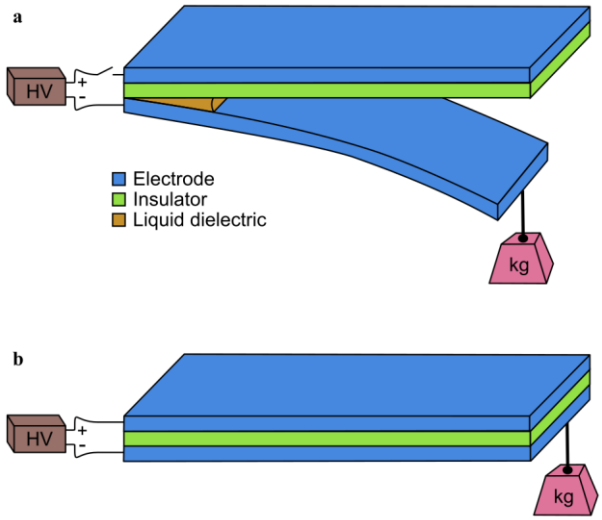

Fig. 2. **a**) Electro-ribbon cantilever test rig, which was used to investigate the effect of insulator and liquid dielectric materials upon DLZ performance. The top electrode and insulator are fixed whereas the bottom electrode is anchored at the left end **b**) Upon application of high voltage, dielectrophoretic liquid zipping along the cantiliver raises the test load.

II. Materials and Methods

Electro-ribbon actuators were fabricated from thin, steel electrodes (1.1274 carbon steel, h+s Präzisionsfoliens GmbH, Germany).

For contraction and self-locking behaviour testing, we fabricated electro-ribbon actuators that were connected at both ends using laser-cut acrylic clamps and nylon nuts and bolts. These "bow-shaped" electro-ribbon actuators flex open like a bow when an external force is applied and close when active, as in Fig. 1b–c. The electrodes were insulated using polyvinyl chloride (PVC) tape (AT7 PVC Electrical Insulation Tape, Advance Tapes, UK). The liquid dielectric was 50 cSt viscosity silicone oil (378356, Sigma-Aldrich, USA).

For materials testing, we used an electro-ribbon cantilever test rig (Fig. 2). The test rig comprised an upper electrode (a 70-µm-thick, 12.7-mm-wide steel strip), attached by adhesive to a horizontal acrylic plate. The upper electrode was insulated using either polyimide tape (tesa 51408, tesa, Germany), polyethylene terephthalate (PET) (639303, Sigma-Aldrich, USA) or the same PVC tape as was used for bow-shaped electro-ribbon actuators. The thickness of the insulator was identical in all cases (130 µm). A second electrode (a 100-µm-thick, 12.7-mm-wide steel strip with free length of 100 mm) was attached to one end of the upper electrode using a laser-cut acrylic clamp and nylon bolts. The addition of a test load to the tip of the second electrode caused cantilever deflection. A droplet of liquid dielectric was introduced at the zipping locus and a high voltage was applied, resulting in dielectrophoretic liquid zipping and raising of the load. A range of liquid dielectrics were used: in addition to the 50 cSt viscosity silicone already described, we also used 5 cSt viscosity silicone oil (317667, Sigma-Aldrich, USA), 500 cSt viscosity silicone oil (378380, Sigma-Aldrich, USA), light mineral oil (330779, Sigma-Aldrich, USA) and heavy mineral oil (330760, Sigma-Aldrich, USA).

All devices were tested isotonically, with a load applied to extend the actuator, and high voltage lifting the load against gravity. During isotonic testing, a known mass was attached to the lower electrode of the actuator, exerting a constant vertical load and extending the device. Variance between different samples has previously been shown to be low for electro-ribbon actuators [13] and therefore was not studied here.

Actuator extension and contraction was recorded using a laser displacement meter (LK-G402, Keyence, Japan). Contraction was calculated by dividing vertical stroke by the total height of the actuator when extended. Liquid dielectric was added by pipette to the device's zipping locus/loci, and high voltage was applied using two high-voltage amplifiers (5HVA24-BP1, UltraVolt, USA). Actuation of electro-ribbon actuators requires very low currents; the maximum current these units could deliver was 200 µA. Control signals and data were output and recorded using a data acquisition device (NI USB-6343, National Instruments, USA).

III. Results and Discussion

A. *Contraction*

Fig. 3 shows results from contraction experiments. A bow-shaped electro ribbon actuator was able to lift an 8 g mass using applied voltages ≥ 5 kV (Fig. 3a). In all cases, the maximum contraction of the actuator was > 99%. Increasing voltage from 5 kV to 10 kV increased the speed of contraction, with full contraction taking 2.5 seconds at an applied voltage of 5 kV, reducing to less than one second at an applied voltage of 10 kV.

Similarly, a bow-shaped actuator was able to lift masses ranging from 8 to 14 g at an applied voltage of 10 kV (Fig 3b). As before, the maximum contraction of the actuator was > 99% in all cases. Increasing the load slightly increased the time taken to reach full contraction.

Electro-ribbon actuators can deliver extremely high contractions over a range of voltage inputs and loads. For applications where high speed is not required, lower applied voltages can be used to do the same mechanical work, improving device safety.

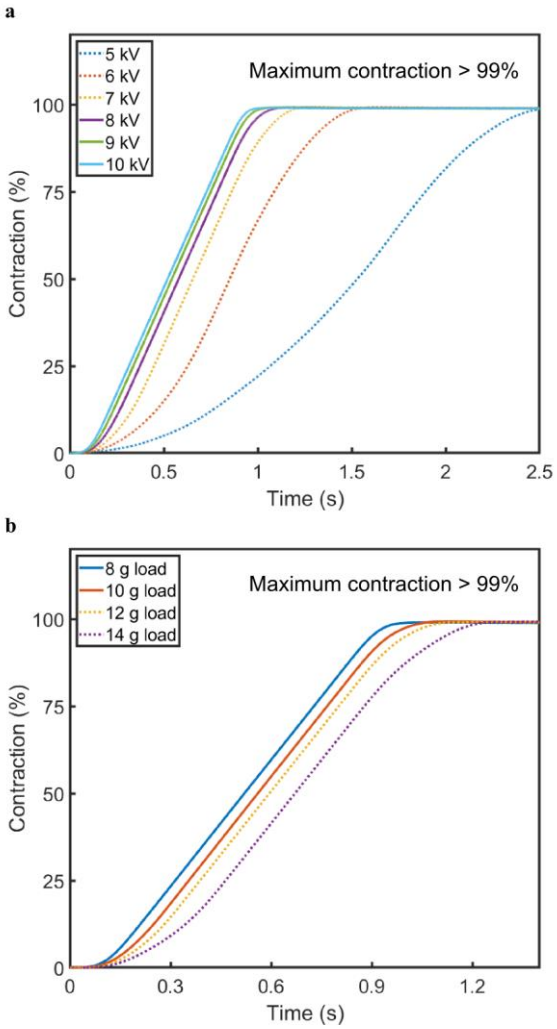

Fig. 3. Isotonic contraction of a bow-shaped electro-ribbon actuator made from 50 µm thick, 100 mm long, 12.7 mm wide electrodes. **a**) Contraction-voltage dependency while lifting an 8 g load. **b**) Contraction-load dependency at an applied voltage of 10 kV.

B. *Self-locking*

Fig. 4 shows results from self-locking experiments. A 17.6-g load was added to the lower electrode of the actuator, and applied voltage was incrementally increased from zero to 8 kV and then reduced gradually back to zero. Applied voltage was held constant at each voltage step for 5 seconds. Actuator contraction increased gradually as voltage was increased, until reaching 8 kV at which point the actuator zipped completely closed, contracting by more than 99%. Applied voltage was then gradually reduced to zero. The actuator remained fully contracted, supporting the 17.6 g mass, even when applied voltage was as low as 0.6 kV. When the voltage was reduced to 0.4 kV, the actuator relaxed.

This self-locking behaviour—the ability of electro-ribbon actuators to deliver a high post-contraction holding force at a fraction of the applied voltage required for full-contraction—has myriad uses in actuating devices. Electro-ribbon-powered solenoids and valves could hold their position after changing state at negligible energy cost, the dominant losses being a

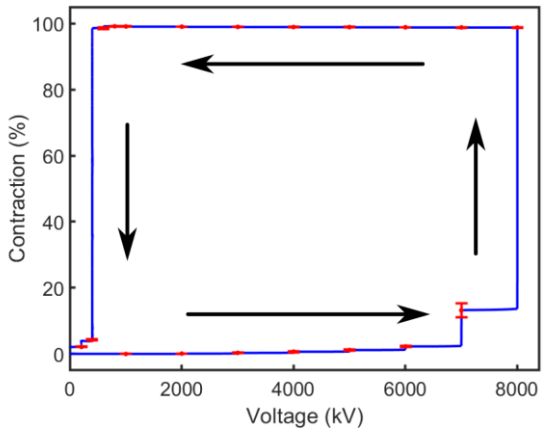

Fig. 4. Isotonic contraction of a bow-shaped electro-ribbon actuator made from 50 µm thick, 100 mm long, 12.7 mm wide electrodes lifting a 17.6 g mass. Voltage was increased and reduced from zero to 8 kV and back. Points are averages of three trials and error bars show ± one standard deviation.

leakage current that flows through the insulator. This leakage current was less than 0.5 μA in self-locking experiments, implying a self-locking power consumption of only 0.3 mW. This is considerably lower than the power consumption of electro-magnetic solenoids and valves, which require current to flow continually to sustain a strong magnetic field in order to exert force. Self-locking electro-ribbon actuators also allow for low-power-consumption variable-stiffness structures, such as electroadhesive clutches that control their stiffness using electrostatic forces between adjacent layers [19].

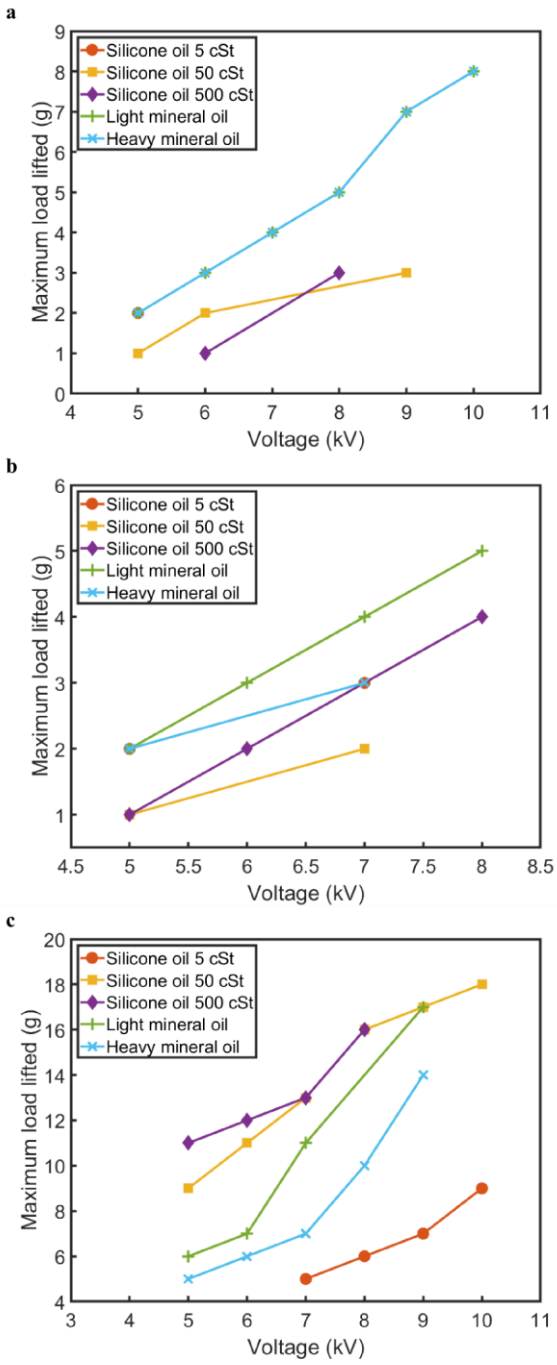

Fig. 5. The effect of applied voltage upon maximum load lifted when using various liquid dielectrics, with **a**) polyimide tape, **b**) PET or **c**) PVC tape as the electro-ribbon actuator insulator material.

The self-locking behaviour of electro-ribbon actuators is a result of pull-in instability; contractile force increases rapidly as the actuator contracts, resulting in a certain contraction below which the actuator will always fully contract at each applied voltage. Despite this property, feedback control of electro-ribbon actuators has been demonstrated [20].

C. Materials study

Fig. 5 shows results from materials testing using the electro-ribbon cantilever test rig. Fig. 5a–c show the maximum load lifted when using a range of liquid dielectric materials for electro-ribbon actuators insulated with polyimide tape, PET and PVC tape respectively. The greatest load that could be lifted for each insulator–liquid-dielectric combination is shown in Fig. 6.

For the choice of insulation, PVC tape resulted in the greatest load lifted, followed by polyimide tape and then PET. The permittivity of PET and polyimide tape are typically stated as 3–3.4 and 3.4–3.5 respectively, while the PVC tape used had a permittivity of 4.62 (personal communication, Advance Tapes). Results indicate that tensile force was greater when using higher permittivity insulators, consistent with (1).

The liquid dielectric that maximises load lifted depends upon the insulator. For polyimide and PET, mineral oil was the best choice, while for PVC tape, silicone oil resulted in the highest load lifted. Hydrocarbon lubrication oils have dielectric constants ranging from 2.1 to 2.8 [21]: mineral oil is typically stated as having a permittivity of 2.1, while the permittivity of 5-cSt, 50-cSt and 500-cSt silicone oil are 2.59, 2.71 and 2.75 respectively [22]. Results indicate that when insulator permittivity is high, higher permittivity liquids allow for greater forces, while when insulator permittivity is low, lower permittivity liquids should be used. This is also supported by (1). If $\varepsilon_{insulator}$ is very large, (1) tends to

$$F = \frac{\frac{1}{2}\varepsilon_{medium}\varepsilon_0 AV^2}{{t_{medium}}^2} \qquad (2)$$

while if $\varepsilon_{insulator}$ is very small, (1) tends to

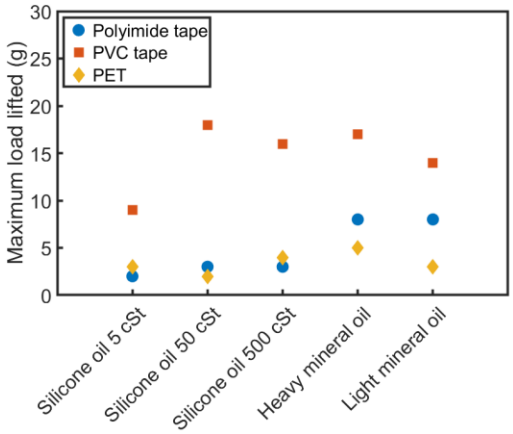

Fig. 6. Absolute maximum load lifted for each insulator–liquid-dielectric combination.

$$F = \frac{\frac{1}{2}\varepsilon_0 A V^2}{\varepsilon_{medium}\left(\frac{t_{insulator}}{\varepsilon_{insulator}}\right)^2} \quad (3)$$

As can be seen from (2)–(3), to maximise tensile force, ε_{medium} (the permittivity of the liquid dielectric) should be large if $\varepsilon_{insulator}$ is very large, but small if $\varepsilon_{insulator}$ is very small.

This can be explained by considering how the electric field is distributed in a capacitor-like system with two nonconducting layers (representing the insulator and the liquid dielectric) in series. The electric field is strongest in the layer with the lower permittivity. If the insulator permittivity is large, the electric field is concentrated in the liquid, and higher permittivity liquids improve tensile force as suggested by Maxwell pressure, $P = \varepsilon E^2$.

In contrast, if the insulator permittivity is small, the electric field is concentrated in the insulator layer where it only induces an electrostatic pressure that compresses the insulator; the electric field in the liquid (which is the field that contributes to electro-ribbon actuator tensile force) is comparatively low. In this case, reducing the liquid permittivity relative to the insulator strengthens the electric field in the liquid layer (and weakens of the electric field in the insulator layer). The effect of reducing permittivity ε upon Maxwell pressure P is more than compensated by the increase in electric field, since $P \propto E^2$, and tensile force is increased.

In addition to permittivity, the breakdown strength of the insulator and liquid dielectric both limit the electric field that may be sustained in the electro-ribbon device, and thus limit performance according to Maxwell pressure. Materials with higher breakdown strength allow stronger fields to be sustained in the actuator, improving tensile force. Finally, nonelectrical properties can also influence performance, such as liquid density and viscosity or fluidic interactions between the insulator surface and liquid dielectric.

IV. Conclusion

Recently developed electro-ribbon actuators are simple, low-cost, scalable electrostatic devices powered by dielectrophoretic liquid zipping that exhibit high efficiency, high power and high contractions exceeding 99%. They can be activated using a range of applied voltages to do work upon various loads, depending on the desired actuation speed.

Self-locking experiments showed that a typical electro-ribbon actuator can hold its actuated state even when voltage is reduced more than tenfold from 8 kV to 0.6 kV. This self-locking behaviour could allow for extremely low-power-consumption solenoids and valves.

Due to materials property interdependence, the constituent materials of electro-ribbon actuators should be carefully selected to maximise tensile force. Results suggest that both insulator and medium permittivity should be high, with insulator permittivity being the greater of the two.

Appendix

TABLE I. Maximum Contraction of Various Actuators

Technology	Maximum contraction (%)
Magnetostrictive	0.2 [4]
Carbon nanotube actuator	1 [23]
Piezoelectric material	1.7 [4]
Electric liquid-crystal elastomer	4 [24]
Electrostrictive material	4.3 [4]
Shape memory alloy	5 [4]
Peano-HASEL	10 [25]
Electroactive gel	18 [26]
McKibben pneumatic actuator	30 [27]
Biological muscle	40 [4]
Pleated pneumatic artificial muscles	42 [28]
Thermal liquid-crystal elastomer	45 [29]
Vacuum-actuated muscle-inspired pneumatic structures	45 [30]
Multilayer stacked dielectric elastomer actuator	46 [12]
Coiled polymer actuator	49 [5]
Traditional pneumatic, hydraulic and linear electromagnetic actuators	50 [4], [31]
High-displacement textile pneumatic artificial muscle	65 [8]
Shape memory polymer	77[a] [1]
Single layer dielectric elastomer actuator	79 [11]
Fluid-driven origami-inspired artificial muscles	90 [9]
Shape-memory alloy coil	92 [2]
Spiral coiled polymer	98.85 [3]
Origami-based vacuum pneumatic artificial muscle	99.7 [10]
Electro-ribbon actuator	99.84 [13]

a. Shape-memory polymers stretched seven times their original length showed up to 90 % strain recovery rate implying contractile strains of 77 %

References

[1] A. Lendlein and S. Kelch, "Shape-Memory Polymers," *Angew. Chemie Int. Ed.*, vol. 41, no. 12, p. 2034, Jun. 2002, doi: 10.1002/1521-3773(20020617)41:12<2034::AID-ANIE2034>3.0.CO;2-M.

[2] S.-M. An, J. Ryu, M. Cho, and K.-J. Cho, "Engineering design framework for a shape memory alloy coil spring actuator using a static two-state model," *Smart Mater. Struct.*, vol. 21, no. 5, p. 055009, May 2012, doi: 10.1088/0964-1726/21/5/055009.

[3] C. S. Haines, N. Li, G. M. Spinks, A. E. Aliev, J. Di, and R. H. Baughman, "New twist on artificial muscles," *Proc. Natl. Acad. Sci.*, vol. 113, no. 42, pp. 11709–11716, Oct. 2016, doi: 10.1073/pnas.1605273113.

[4] P. Brochu and Q. Pei, "Advances in dielectric elastomers for actuators and artificial muscles," *Macromol. Rapid Commun.*, vol. 31, no. 1, pp. 10–36, 2010, doi: 10.1002/marc.200900425.

[5] C. S. Haines *et al.*, "Artificial Muscles from Fishing Line and Sewing Thread," *Science (80-.).*, vol. 343, no. 6173, pp. 868–872, Feb. 2014, doi: 10.1126/science.1246906.

[6] I. W. Hunter, S. Lafontaine, J. M. Hollerbach, and P. J. Hunter,

"Fast reversible NiTi fibers for use in microrobotics," in *[1991] Proceedings. IEEE Micro Electro Mechanical Systems*, 1991, pp. 166–170, doi: 10.1109/MEMSYS.1991.114789.

[7] S. Song, J. Lee, H. Rodrigue, I. Choi, Y. J. Kang, and S.-H. Ahn, "35 Hz shape memory alloy actuator with bending-twisting mode," *Sci. Rep.*, vol. 6, no. 1, p. 21118, Aug. 2016, doi: 10.1038/srep21118.

[8] H. D. Yang, B. T. Greczek, and A. T. Asbeck, "Modeling and Analysis of a High-Displacement Pneumatic Artificial Muscle With Integrated Sensing," *Front. Robot. AI*, vol. 5, no. January, pp. 1–13, Jan. 2019, doi: 10.3389/frobt.2018.00136.

[9] S. Li, D. M. Vogt, D. Rus, and R. J. Wood, "Fluid-driven origami-inspired artificial muscles," *Proc. Natl. Acad. Sci.*, vol. 114, no. 50, pp. 13132–13137, Dec. 2017, doi: 10.1073/pnas.1713450114.

[10] J.-G. Lee and H. Rodrigue, "Origami-Based Vacuum Pneumatic Artificial Muscles with Large Contraction Ratios," *Soft Robot.*, vol. 6, no. 1, pp. 109–117, Feb. 2019, doi: 10.1089/soro.2018.0063.

[11] L. J. Romasanta, M. A. Lopez-Manchado, and R. Verdejo, "Increasing the performance of dielectric elastomer actuators: A review from the materials perspective," *Prog. Polym. Sci.*, vol. 51, pp. 188–211, Dec. 2015, doi: 10.1016/j.progpolymsci.2015.08.002.

[12] G. Kovacs, L. Düring, S. Michel, and G. Terrasi, "Stacked dielectric elastomer actuator for tensile force transmission," *Sensors Actuators A Phys.*, vol. 155, no. 2, pp. 299–307, 2009.

[13] M. Taghavi, T. Helps, and J. Rossiter, "Electro-ribbon actuators and electro-origami robots," *Sci. Robot.*, vol. 3, no. 25, p. eaau9795, Dec. 2018, doi: 10.1126/scirobotics.aau9795.

[14] L. Maffli, S. Rosset, and H. R. Shea, "Zipping dielectric elastomer actuators: characterization, design and modeling," *Smart Mater. Struct.*, vol. 22, no. 10, p. 104013, 2013, doi: 10.1088/0964-1726/22/10/104013.

[15] A. S. Chen, H. Zhu, Y. Li, L. Hu, and S. Bergbreiter, "A paper-based electrostatic zipper actuator for printable robots," in *2014 IEEE International Conference on Robotics and Automation (ICRA)*, 2014, pp. 5038–5043, doi: 10.1109/ICRA.2014.6907597.

[16] J. Li, H. Godaba, Z. Q. Zhang, C. C. Foo, and J. Zhu, "A soft active origami robot," *Extrem. Mech. Lett.*, vol. 24, pp. 30–37, Oct. 2018, doi: 10.1016/j.eml.2018.08.004.

[17] Z. Suo, "Theory of dielectric elastomers," *Acta Mech. Solida Sin.*, vol. 23, no. 6, pp. 549–578, Dec. 2010, doi: 10.1016/S0894-9166(11)60004-9.

[18] H. Pellat, "Électrostatique non fondée sur les lois de coulomb. Forces agissant sur les diélectriques non électrisés," *J. Phys. Théorique Appliquée*, vol. 5, no. 1, pp. 244–256, 1896, doi: 10.1051/jphystap:018960050024401.

[19] S. Diller, C. Majidi, and S. H. Collins, "A lightweight, low-power electroadhesive clutch and spring for exoskeleton actuation," in *2016 IEEE International Conference on Robotics and Automation (ICRA)*, 2016, vol. 2016-June, pp. 682–689, doi: 10.1109/ICRA.2016.7487194.

[20] S. Bluett, T. Helps, M. Taghavi, and J. Rossiter, "Self-sensing Electro-ribbon Actuators," *IEEE Robot. Autom. Lett.*, 2020.

[21] A. A. Carey, "The Dielectric Constant of Lubrication Oils," vol. 34, no. 11, 1998.

[22] CLEARCO, "Dielectric Properties of Pure Silicone Fluids," 2013.

[23] R. H. Baughman, "Carbon Nanotube Actuators," *Science (80-.).*, vol. 284, no. 5418, pp. 1340–1344, May 1999, doi: 10.1126/science.284.5418.1340.

[24] W. Lehmann *et al.*, "Giant lateral electrostriction in ferroelectric liquid-crystalline elastomers," *Nature*, vol. 410, no. 6827, pp. 447–450, Mar. 2001, doi: 10.1038/35068522.

[25] N. Kellaris, V. Gopaluni Venkata, G. M. Smith, S. K. Mitchell, and C. Keplinger, "Peano-HASEL actuators: Muscle-mimetic, electrohydraulic transducers that linearly contract on activation," *Sci. Robot.*, vol. 3, no. 14, p. eaar3276, Jan. 2018, doi: 10.1126/scirobotics.aar3276.

[26] T. Helps, M. Taghavi, and J. Rossiter, "Thermoplastic electroactive gels for 3D-printable artificial muscles," *Smart Mater. Struct.*, Dec. 2018, doi: 10.1088/1361-665X/aafa5a.

[27] B. Tondu and P. Lopez, "Modeling and control of McKibben artificial muscle robot actuators," *IEEE Control Syst.*, vol. 20, no. 2, pp. 15–38, Apr. 2000, doi: 10.1109/37.833638.

[28] F. Daerden, D. Lefeber, B. Verrelst, and R. Van Ham, "Pleated pneumatic artificial muscles: actuators for automation and robotics," *2001 IEEE/ASME Int. Conf. Adv. Intell. Mechatronics. Proc. (Cat. No.01TH8556)*, vol. 2, no. July, pp. 738–743, 2001, doi: 10.1109/AIM.2001.936758.

[29] D. K. Shenoy, D. Laurence Thomsen III, A. Srinivasan, P. Keller, and B. R. Ratna, "Carbon coated liquid crystal elastomer film for artificial muscle applications," *Sensors Actuators A Phys.*, vol. 96, no. 2–3, pp. 184–188, Feb. 2002, doi: 10.1016/S0924-4247(01)00793-2.

[30] D. Yang *et al.*, "Buckling Pneumatic Linear Actuators Inspired by Muscle," *Adv. Mater. Technol.*, vol. 1, no. 3, p. 1600055, Jun. 2016, doi: 10.1002/admt.201600055.

[31] J. M. Hollerbach, I. W. Hunter, and J. Ballantyne, "A comparative analysis of actuator technologies for robotics," in *The Robotics Review*, vol. 2, 1991, pp. 299–342.